Effect of build orientation and post-curing of (meth)acrylate-based photocurable resin fabricated by stereolithography on the mechanical behavior from quasi-static to high strain rate loadings

Mohammadali Shirinbayan[1] · Nader Zirak[1,2] · Ouiza Saddaoui[2,3] · Amrid Mammeri[3] · Kamel Azzouz[3] · Khaled Benfriha[4] · Abbas Tcharkhtchi[1] · Joseph Fitoussi[1]

Abstract
Stereolithography (SLA) is becoming an important fabrication method among the different additive manufacturing techniques. This study investigates the effect of high strain rate on mechanical behavior, considering the fact that materials can be shown different mechanical properties under rapid straining compared to quasi-static loading. In addition, the role of polymerization as a determining factor in the final mechanical properties of the SLA parts is indicated. Regarding that, samples based on urethane dimethacrylate resin material were printed in different directions ($\theta = [0–90]$) and post-treatment was performed with respect to the UV and UV with temperature. The effect of high strain rate was analyzed through a servo-hydraulic machine, monotonic, and interrupted tensile tests ranging from 0.3 to 117.4 s^{-1}. Scanning electron microscopy was applied to analyze the failure surface characteristics. The results show the important effect of strain rate on mechanical properties such that by increasing the strain rate, yield stress and ultimate stress were increased. Furthermore, investigation of the strain rate sensitivity during the different steps of the failure indicates more sensitivity of the non-linear zone of the stress–strain curve with strain rate.

Keywords Additive manufacturing · Stereolithography manufacturing · Polymers (durable resin) · Mechanical behavior · High strain rate

1 Introduction

Additive manufacturing has attracted a lot of attention considering the fabrication of complex geometry and economic efficiency [1–4]. Among the different manufacturing methods, stereolithography considering the good precision, economic efficiency, easiness of printing of parts, and providing the ability to innovative new products has been at the center of a lot of studies [5]. Different applications of this technique across a wide range of industrial sectors such as

✉ Nader Zirak
nader.zirak@ensam.eu

Mohammadali Shirinbayan
mohammadali.shirinbayan@ensam.eu

Ouiza Saddaoui
ouiza.saddaoui@ensam.eu

Amrid Mammeri
amrid.mammeri@valeo.com

Kamel Azzouz
kamel.azzouz@valeo.com

Khaled Benfriha
khaled.benfriha@ensam.eu

Abbas Tcharkhtchi
abbas.tcharkhtchi@ensam.eu

Joseph Fitoussi
joseph.fitoussi@ensam.eu

[1] Arts Et Metiers Institute of Technology, CNAM, PIMM, HESAM University, 75013 Paris, France

[2] Arts Et Metiers Institute of Technology, CNAM, LIFSE, HESAM University, F-75013 Paris, France

[3] Valeo Thermal Systems, 8 rue Louis Lormand, La Verriere, 78322 Le Mesnil ST Denis Cedex, France

[4] Arts Et Metiers Institute of Technology, CNAM, LCPI, HESAM University, Paris, France

automobiles, medical, and aerospace industry have led to more and more research in this area [6].

In this method, polymerization of a photocurable liquid resin can happen through exposure to ultraviolet laser radiation and subsequently lead to solid objects. Fabrication of the parts is in layer by layer of cured resin. The passage of the laser according to the pre-determined design causes the formation of solid layers mounted on a platform immersed in the resin bath. The curing of the resin during the fabrication is accompanied by entrapped uncured monomers between the solid layers. In general, curing up to 65% can be achieved considering the kind of polymer and laser source in the samples during the process [7]. There are a lot of parameters that can impact the final part properties; nevertheless, the percentage of curing and orientation of printing have been among the key parameters that changed the properties such as the mechanical behavior of the parts.

Chantarapanich et al. [8] studied the main build orientations (flat and edge) and sub-build orientations (0°, 45°, and 90° with respect to the *x*-axis) on mechanical properties. Their results showed the important effect of main build orientation on elastic modulus, UTS, elongation at UTS, and elongation at break, whereas this effect was not significant for different sub-build orientations. In another work, anisotropy due to the different print orientations shows the importance of this parameter on the mechanical properties. Regarding that, it has been shown that the difference in elongation of a sample positioned in the YZ plane with the axis of the specimen orientated in the Y-direction and printed sample in the YZ plane with the axis of in the Z-direction was 8% [9].

The effect of residual monomers in the parts is such that it can have a significant impact on the final properties of products [10]. Therefore, post-processing consisting of washing and post-curing was essential to decrease the quantity of unreacted monomers [11]. Generally, in washing, printed parts are immersed in a suitable solvent for quitting the unreacted monomers from solid parts. Another way to decrease the amount of unreacted monomers is post-curing the residual monomers. In this method, curing of the residual monomers can be happened through heating, microwave, and exposure of the produced sample against UV radiation by the conventional oven, microwave oven, and ultraviolet chamber. Among the techniques of post-curing, using UV post-treatment has been mentioned as a method with the ability to increase the mechanical resistance to the maximum amount [12]. Furthermore, a chamber with high-intensity ultraviolet with the ability to heat the sample which is called post-curing apparatus has been used in many studies [13]. Depending on the time and heating, different cured percents can be achieved in the samples.

Investigation of the mechanical behavior of the material in severe conditions has been subjected in center of many studies [14–16]. Considering the time-dependence mechanical behavior of polymers, dependence of elastic modulus and yield strength is expected. So, different responses of polymers respected to the various loading that refers to the sensitivity of the polymers with strain rates have attracted a lot of attention [16–18]. Table 1 investigates the effect of strain rates on the polymeric materials according to the different studies. The change in the mechanical response is such that can be transformed from rubbery to ductile plastic to brittle. So, understanding the mechanism of damage can play a vital role during experiment with different strain rates [19]. Resistance to polymer chain alignment in the high strain point can create strain hardening which will be balanced during the test. This balancing can be performed through adiabatic heating [20, 21]. Regarding that, extensive studies have been done on investigating the effect of strain rate in the compressive state on polymers [22–24]. In general, the experiments of compressive tests in high strain showed the increasing of modulus and yield stress with rising the strain rate with a brittle fractured [25]. On the other hand, due to the more difficulties of the tensile test compared to the competition, fewer studies have been performed in this state. Gilat et al. [26] studied the two different types of epoxy of E-862 and PR-520 which are non-toughened two-part, and one-part toughened epoxy resin, respectively, in the different loading conditions at 5×10^{-5}, 2 and 450–700 s^{-1}. Their results showed an important effect of strain rate on the maximum shear stress, such that it was increased by increasing the strain rate. Somarathna et al. [27] investigated polyurethane as an elastomeric polymer at different strain rates from 0.001 to 0.33 s^{-1}. Their results emphasized increasing the mechanical behavior such as Young's module, yield stress, ultimate tensile stress, and failure stress with increasing the strain rates. Increasing the ultimate tensile stress of the samples was attributed to the stiffness with increasing strain rates. Also, the strain energy density of samples showed the dependency on the strain rate, that a higher strain rate was accompanied by the lower absorbed energy.

The objective of this study is to investigate the effect of fabrication process parameters and post-processing of stereolithography technique on mechanical behavior. Different build orientations and post-treatment conditions were considered for the fabrication of the parts. Mechanical characterization was performed under the condition of quasi-static to high strain loadings. The strain rates were 0.001, 0.3, 4.6, and 117.4 s^{-1} and the ultimate stresses were obtained 36.6, 67.5, 68.8, and 73 MPa, respectively. In addition, the fracture surface was probed through scanning electron microscopy. The results of microscopy show changes in the morphology of fracture, such that the plastic deformation zone disappears with increasing the strain rate. Fracture samples

Table 1 Effect of strain rates on the different polymers

Material	Samples fabrication method	Dynamic loading	Strain rate (s^{-1})	Results	Ref
Polycarbonate and polyvinylidene difluoride	Injection molding	Split Hopkinson pressure bar	10^{-4}–10^{4}	An extreme increase in yield strength by enhancement of the strain rate was shown and was referred to as the movement of the b transition to room temperature at these rates	[31]
Polymethylmethacrylate	Machining	Servohydraulic axial testing machine	0.1–0.001	Increasing the temperature in the strain rate of 0.01/s and 0.1/s was lead to the thermal softening of the polymer	[20]
Commercial poly-vinylidene fluoride grade	Machining from extruded parts	Uniaxial tensile	0.005–1	Stress levels increased with increasing strain rate. Plastic dilation was observed at the microscale and enhanced with increasing deformation	[32]
Epoxy	Molding	Split Hopkinson bar	0.001–5100	A high dependency of mechanical properties with strain rate was shown. Stress–strain curves with respect to the different strain rates can be followed by peak stress, subsequently post-yielding stress softening, and strain hardening deformation in the end	[33]

of 4.6 s^{-1} and 117.4 s^{-1} showed a brittle breaking, including increasing the rate of strain led to crack growth instead of increasing crack density.

2 Material description, 3D printer device, and characterization methods

2.1 Raw material

A Photocurable resin, Black Resin, with product code of FLGPBK04 from Formlabs (Berlin, Germany) was used as a raw material. The resin has consisted of urethane dimethacrylate diluted with the corresponding methacrylate monomers, and bis(2,-4,6 trimethylbenzoyl) phenylphosphine oxide as a photoinitiator. Also, isopropyl alcohol 99.9% was used during post processing.

2.2 Samples fabrication

Samples were printed with a Formlabs 3D printer. The process of printing consisted of importing the geometry to the slicer in order to create the G-cod and then bring it to the 3D printer. Samples were printed with a Formlabs 3D printer. The geometry of samples for mechanical tests is shown in Fig. 1. The stated technical considerations for printing the parts are shown in Table 1. Figure 2 shows the samples that were printed in different build orientations. After printing the parts, support was detached and post-processing was performed. Post-processing in this study consisted of two processes of washing and post-treatment that were performed through the form wash and form cure, respectively. The time of washing was set to 30 min for all the samples. Post-curing of samples was in the presence of UV at different heating temperatures of 50, 60, and 80 °C for 30 min. In order to reduce perturbation and disturbance wave's impact on the sample, and obtain homogenous strain flowing, ABAQUS FE optimization was applied and then the best fit geometry was proposed. In addition, this optimization is accompanied by rapid stabilization of strain rate in the sample gauge part during the first stage of applying load during the test [28, 29].

Fig. 1 Dimensions of specimen for tensile test

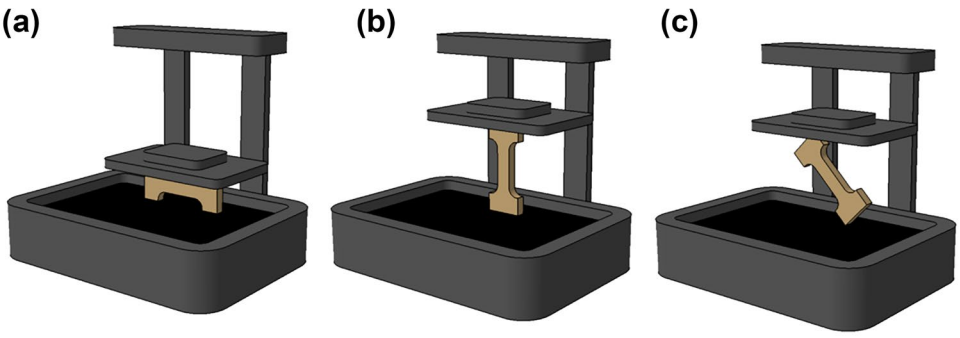

Fig. 2 Schematic of different build orientation direction of samples printing: **a** 0°, **b** 90°, and **c** 45°

2.3 Methods of characterization and experimental procedure

2.3.1 Microscopic observation

The fracture surfaces of the samples were analyzed by a scanning electronic microscope (HITACHI 4800 SEM). Regarding after the test in different stain rates, samples were coupled from the fractured side and were analyzed.

2.3.2 Differential scanning calorimetric

In order to analysis the percentage of curing the samples, differential scanning calorimetric (DSC) was used (Q1000 V9.0 Build 275 DSC, TA instrument). The test was carried out on resin and the green and post cured printed samples. Approximately 8 g of printed samples was separated, while capsule was prepared for 5 g uncured resin. The thermogram heating was selected from 50 up to 210 °C with heating rate of 10 °C/min.

2.3.3 Quasi-static tensile test

A low-speed tensile test was performed for specimens printed for different sub-build orientations without and with different post-curing conditions. Regarding that, MTS 830 hydraulic machine with a loading cell of 10 kN used, the constant ramp speed was set at 5 mm/min. The repetitively of each test was checked out by using 4 samples.

In order to investigate the different strain rates from quasi-static to 117.5 s^{-1}, a servo-hydraulic machine as specified by the manufacturer (Schenk Hydropuls VHS 5020) was applied. The load level was measured by a crystal 50-kN load cell during the experiment. Figure 3 illustrates the schematic of this equipment; as can be seen, the samples were placed between the load cell and the moving device.

2.3.4 High strain tensile loading characterizations

To understand the global mechanical behavior and related damage mechanisms of printed samples, tension loading with different strain rates was applied. Regarding our last investigations [29, 30] of the high strain rate tensile test, for experimental evaluation of strain–time measurement, 2 points were put on the face of the sample for defining the initial gauge in the tension test, and then changes were monitored via a high-speed camera. Subsequently, image analysis was used to observe a displacement of the centroid of each marked point to show the strain between the two points. Regarding tdhe simulation and experimental results, it was proved that after the damping stage, the strain rate became constant that consequently could be measured from the slope of the linear part of the curve in Fig. 4, which is a confirmation of the chosen boundary conditions in accordance with ABAQUS FE simulation.

3 Experimental results and discussion

3.1 Curing percentage

In order to investigate the curing percentage afer fabrication the parts, DSC analysis was performed. Figure 5 shows the

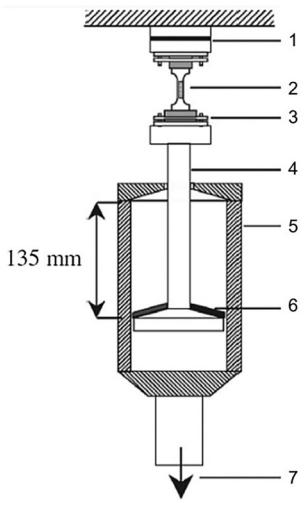

Fig. 3 Schematics of high strain-rate tensile test: 1, load cell; 2, sample; 3, fixing system; 4, sliding bar; 5, hydraulic jack; 6, damping joint; and 7, displacement direction

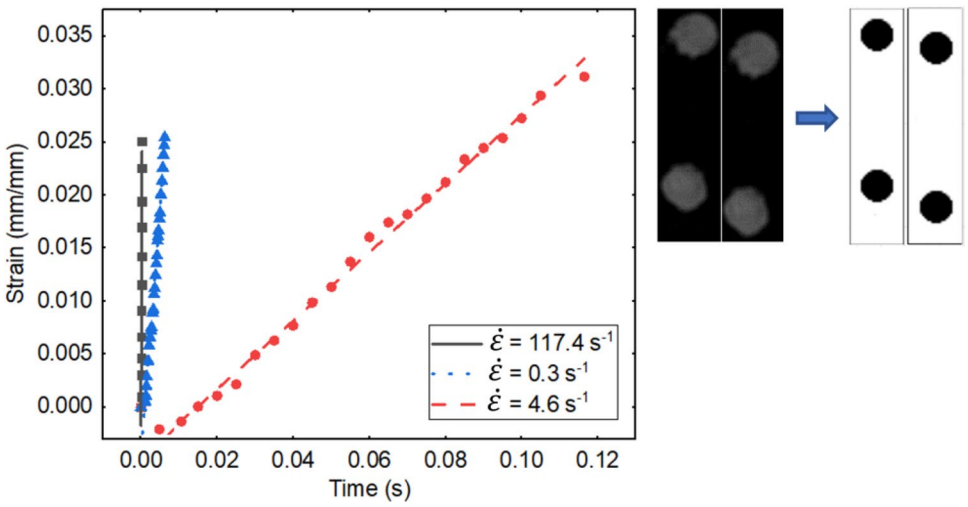

Fig. 4 Strain measurements against the time

results of DSC for different samples in green and different post curing conditions. Exothermic picks that appeared in the range of 45 to 220 °C is related to the absorbed energy of monomers for polymerization. The area of each peak is related to this energy that is reduced from green to UV + Heat cured at 80 °C. This phenomenon is shown that the less unreacted resine is remanied by post curing. Percentage of curing in each sample was calculated from the following equation:

$$Degree\ of\ cure\ (\%) = (1 - \Delta Hsample/\Delta Hresin) \times 100 \quad (1)$$

where ΔH_{sample} and ΔH_{resin} are the heat release energy from samples and resin, respectively.

Table 2 shows the curing percentage of each sample. According to the results, the lest and most one were 88 and 97.5% that related to the green and UV + Heat cured at 80 °C, respectively. Curing in the resins through the SLA method can happen in two ways: radiation and heating. So, using the UV can cause the curing in the samples. Also, increasing the temperature is accompanied with increasing the chain mobility in the polymers that can enhance the polymerization. So more heating can cause the more curing in the samples during the post treatment.

3.2 Quasi-static tensile behavior

3.2.1 Effect of build orientation: 0°, 45°, 90°

The results from tensile tests are shown in Fig. 6. These results show the stress–strain curve of samples with respect

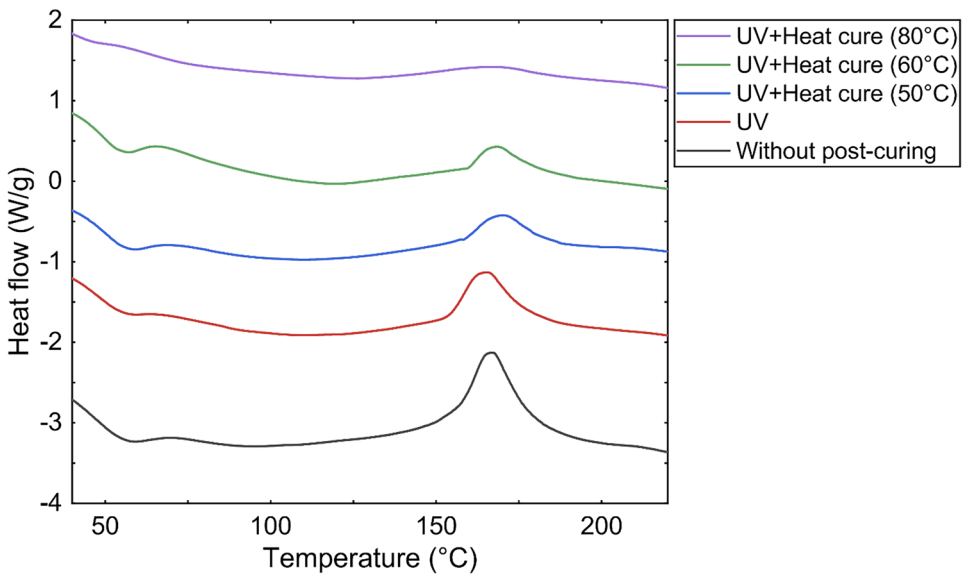

Fig. 5 The results of DSC for the samples

Table 2 Heat release energy and curing percentage of samples

Sample	Heat release energy (J/g)	Curing percentage (%)
Without post-curing	11.9	88.0
UV	10.2	89.7
UV + Heat cure (50 °C)	4.7	95.3
UV + Heat cure (60 °C)	4.1	95.9
UV + Heat cure (80 °C)	2.5	97.5

to the sub build orientation and different post-curing conditions. For investigation of the printing orientation effect on mechanical properties, each printed group in 0°, 45°, and 90° was compared together.

Various directions of printing show the different mechanical behavior of samples. This fact shows the anisotropy of fabricated parts and also can impact the steps up to break in the stress–strain curves. The stress–strain curves for 0°-printed show the linearly elastic, nonlinearly ascending, yield-like (peak) behavior, strain softening, and then plastic flow. These samples indicate the most percentage of elongation compared to the other printed samples in different directions. Literature has shown the plasticizer effect of unreacted monomers on the final product. Also, considering the DSC results that were discussed in the previous section, the amount of residual resin in the samples was shown. So considering the direction of tension, which has been in the direction of the printed plate, it can be said that the elongation of the samples has reached its maximum value. After stretching the material up to the special ratio that is called the "natural draw ratio," necking will be stopped, and through the new material at the neck shoulders, this part starts to grow. This phenomenon, "drawing," continues until it spans the full gauge length of the specimen. Considering the strengthened microstructure during this process, it can be said that failure occurs when new materials are unable to transform outside the neck [10].

Ductile stress–strain curves were observed for 45°-printed samples. According to this figure, the results show the linear elastic and then the plastic flow of samples during the tensile test. The percentage of elongation was less than the 0°-printed samples, while the value of maximum stress at

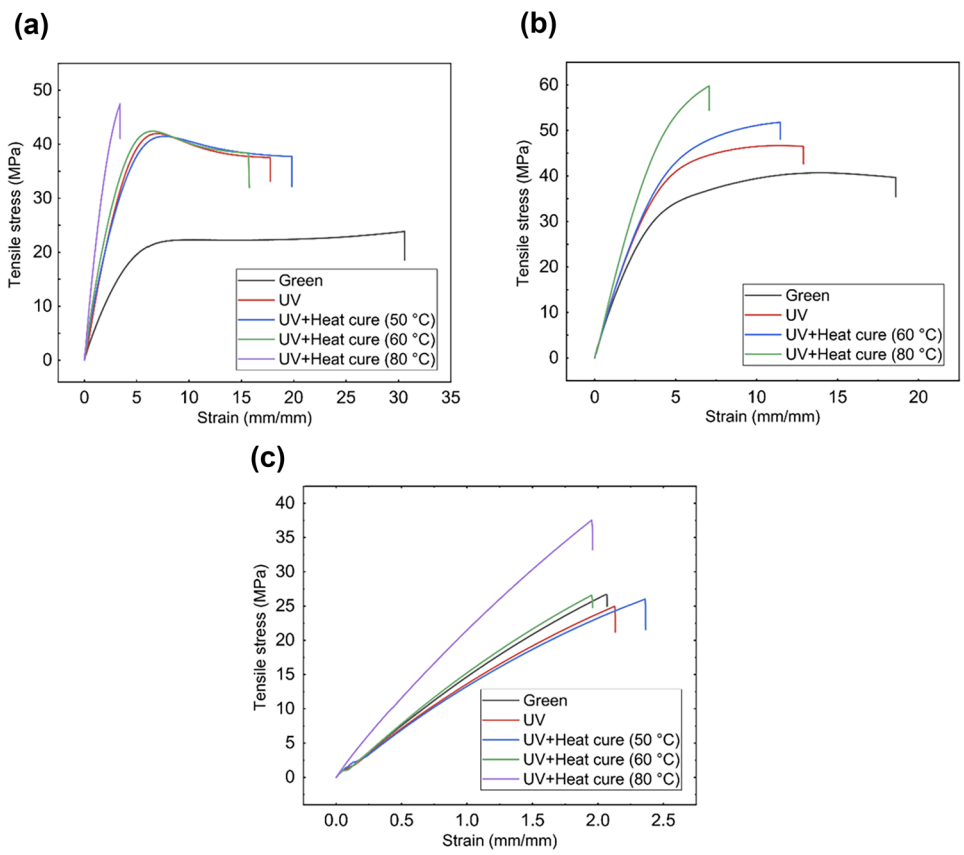

Fig. 6 Stress–strain curves with different post-curing conditions: **a** 0°-printed, **b** 45°-printed, and **c** 90°-printed

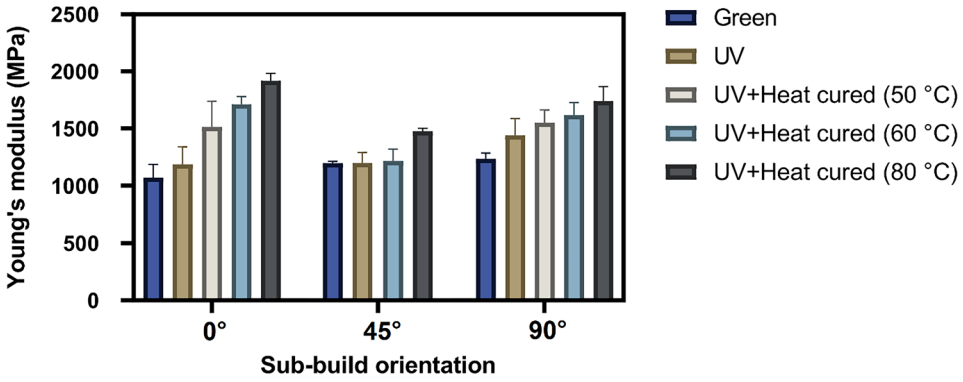

Fig. 7 Young's modulus for green and post-cured samples

break was increased compared to the other two groups. Considering the direction of printed plates with tensile direction in this group, it can be said that material transfer has not occurred in the neck area. This fact caused decreasing elongation. Curves in the group of 90°-printed samples were rigid. This sub-build direction showed the least value in %elongation around 2% and maximum stress at break. In general, the results show that maximum stress at the break for printed samples can be ranked as follows: 45° > 0° > 90°. This fact shows the important effect of sub-build on printing the parts.

3.2.2 Effect of post-curing temperature: 50 °C, 60 °C, and 80 °C

In this section, importance of post curing temperature with UV was analyzed on the samples printed with different build orientations. Figure 7 shows the values of Young's modulus obtained from the mechanical tests. Results showed the important effect of temperature during the post curing on the mechanical behavior, such that Young's modulus of the samples was increased by increasing the temperature. The maximum of the mechanical strength was achieved at 80 °C + UV post treatment in all the printing orientations. This increase can be attributed to the increasing of the curing percentage at high temperatures post curing. The more curing percentage at higher temperature is related to the better mobility of polymeric chains.

Also, according to the results from Fig. 7, the key role of temperature on the shape of stress–strain curves can be observed. In this figure, strain softening effect was reduced by increasing the temperature during the tensile test, especially in the samples printed at 45°. This observation can be explained by the plasticizer effect of residual resin during the test. In addition, increasing the cross-link density can lead to less ability of chains to the movement that leads to the reduction of the strain softening.

3.3 Effect of strain rate on tensile loading: 45°, post-cured

Investigation of strain rate was carried out on the samples of 45°-printed that were post-cured at 80 °C in the presence of UV for 30 min. Figure 8 shows strain–stress curves of this test at different rates from 0.3 to 117.4 s^{-1}. According to the results, the ultimate tensile strength was increased by increasing the rate, such that these values for rates of 117.4, 4.6, and 0.3 s^{-1} were 73, 68.8, and 67.5 MPa, respectively. The different zones of these curves consisted of an initial linear elasticity domain, followed by a yielding domain and then a moderate increase of stress. In addition, the curves of stress–strain did not show a significant change in the slope of elastic zone which can indicate Young's modulus is independent of rates. Stress–strain curve of the similar sample in static condition (0.001 s^{-1}) shows the ductile deformation

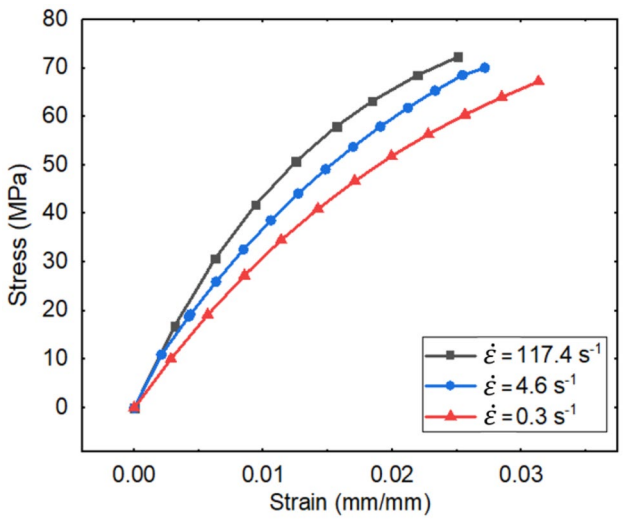

Fig. 8 Stress–strain curves at different strain rates

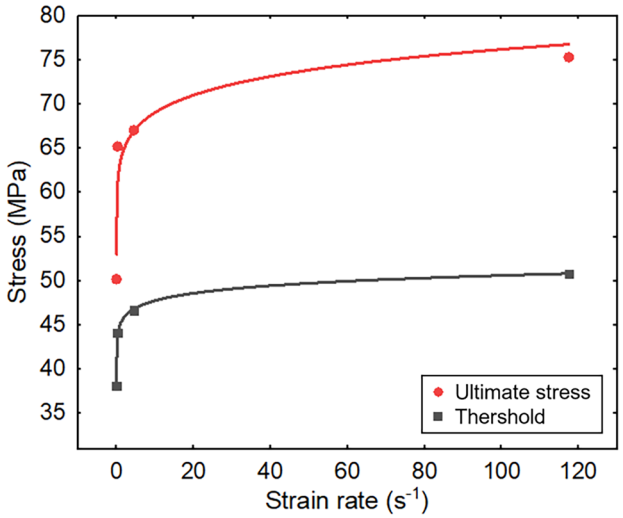

Fig. 9 Strain rate sensitivity for thershold and ultimate stress

with large straining and a low increase of stress. The maximum values of ultimate tensile stress and the strain at break were 59.1 MPa and 6.8%, respectively. So, dynamic loading on the samples caused reducing significantly of strain at break and increased the ultimate tensile stress.

Furthermore, a threshold in the ultimate stress and strain was considered that is corresponding to the first non-linearity behavior. This point can be referred to as a transition from passing linear to nonlinear properties and can be caused by the initial microfracture. Increasing the force during the test, the initial microfracture grew and led to fracture. The stress and strain threshold results are presented in Fig. 9. According to this figure, stress and strain thresholds were decreased by increasing the rate that is described as follows: increasing the rate is accompanied by going to the non-linear stage in less strain and stress. On the other hand, a decrease in the rate can cause the delay of this transition in the samples which means a delayed damage onset. It seems that in the high rate, increasing the rate can cause an increase in the crack density, whereas decreasing the rate can provide more crack propagation. In addition, the results show a direct relation between modulus and strain rate, such that a higher modulus is followed at more strain rates.

Also, for investigation of the failure mechanism and dynamic analysis properties with respect to the effect of strain rate on the stress, strain rate sensitivity "m" was considered. Regarding that, this parameter was evaluated from Backofen equation which is an empirical power-law function, as follows [34]:

$$\sigma = C + K\dot{\varepsilon}^{m} \tag{2}$$

Table 3 Parameters from Backofen equation

Parameters of power function	C	K	m	R^2
Thershold	10.56	34.56	0.03	0.99
Ultimate stress	43.46	20.10	0.11	0.92

where σ is the stress, $\dot{\varepsilon}$ indicates the strain rate, C and K are the constants that referred to the experimental conditions and microstructure of materials, and m shows the SRS index. It can be said that by increasing the SRS index, the sensitivity of the material with strain rate will be raised. Threshold and ultimate stress were considered for investigating the effect of different rates on the different steps of failure, such that sensitivity index from the threshold can correspond to the linear zone, whereas the index from the equation respected to the ultimate stress can refer to the non-linear step. The results from the fitting are shown in Table 3. According to the results, the samples showed more rate sensitivity in the non-linear stage compared to the linear step. This can be attributed to the visco damage behavior of the samples during the test. After the linear stage, the mechanism of the damage will be active which is accompanying the creation of cracks in the samples and is more sensitive to strain rate.

According to the results, a greater m index for ultimate stress compared to the yield stress can show more sensitivity of the sample with strain rate after yield stress, which is located in the zone of non-linear. So, it can be said that the non-linearity stage is more sensitive to strain rate compared to the linear step in the stress–strain curve.

3.4 Fractography

In order to investigate the effect of different strain rates on damage, surface fractures of samples 45°-printed post-cured at 80 °C were observed. Figure 10 shows the SEM of fractured samples in the strain rates of 0.3, 4.6, and 117.4 s^{-1} at different magnifications. The figures show the brittle fracture containing the plastic region which this region will be decreased by increasing the strain rate, such that surface fracture at the strain rate of 117.4 s^{-1} did not show the plastic deformation. Figures 10 a and b are attributed to the strain rate of 0.3 s^{-1}, as can be seen, the cracks have grown more compared to the other strain rates. In addition, according to the shear and cavitation evidence in the plastic area, it can be seen the chain slippage mechanics as a failure mechanism. This mechanism can occur when propagation speed is reduced by the stress release.

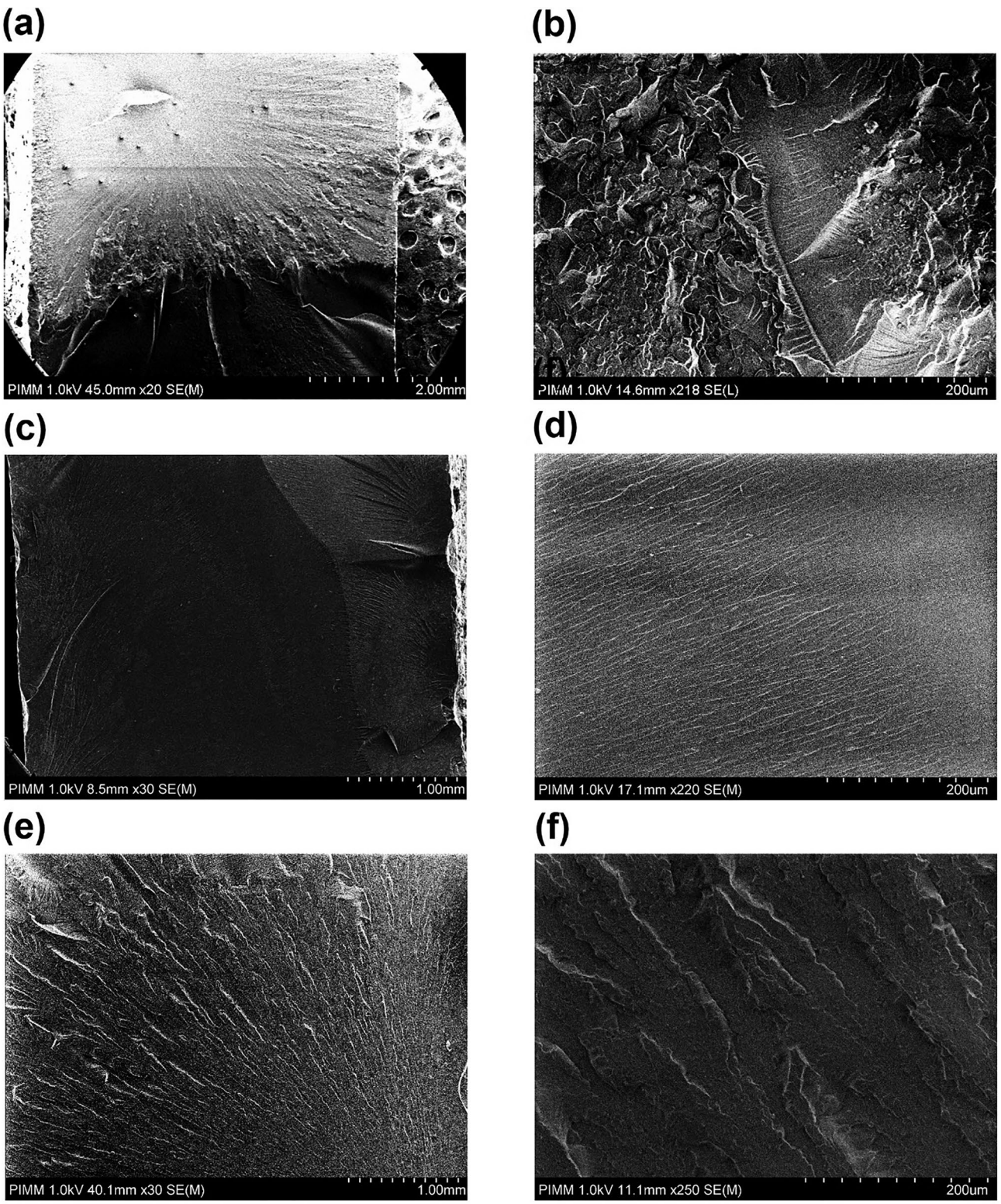

Fig. 10 Surface electron microscopic analysis in different magnification for failure surface at different strain rates: **a**, **b** 0.3 s^{-1}; **c**, **d** 4.6 s^{-1}; and **e**, **f** 117.4 $s^{-.1}$

4 Conclusions

In this study, the effect of build orientation and post-curing in printed samples with SLA was considered. Mechanical properties of the materials were considered under the quasi-static and high strain rate tensile loading. The following points can be concluded:

- The importance of post-curing on final mechanical behavior was shown in the post-processing method. Post curing was accompanied by reducing the residual monomer, such that by increasing the polymerization in the parts elongation was reduced. DSC results show the maximum cure degree of the samples up to 98% during the post-treatment with UV at 80 °C.
- The mechanical behavior of the samples in quasi-static conditions shows the sensibility with build orientation, such that the most value of stress at break was attributed to the 45°-printed parts, then for 0° and finally for 90°. In addition, different shapes in the stress–strain curve consist of brittle, ductile, and curve with softening effect.
- Results of high strain rate from 0.001 to 117.4 s^{-1} on the mechanical behavior show the important role of strain rate on the mechanism of failure. The samples showed more sensibility in the nonlinearity zone compared to the linear step of the stress–strain curves.

Acknowledgements The authors thankfully acknowledge Valeo company support.

Availability of data and material The raw/processed data required to reproduce these findings will be made available on request.

Declarations

Ethics approval The authors are obliged to all the rules regarding the ethics in publication.

Consent to participate This study is not a human transplantation study. No consent is needed for this paper.

Consent for publication The authors consent the policy of publication in the International Journal of Advanced Manufacturing Technology**.**

Competing interests The authors declare no competing interests.

References

1. Ligon SC, Liska R, Stampfl J, Gurr M, Mülhaupt R (2017) Polymers for 3D printing and customized additive manufacturing. Chem Rev ACS Publications 117:10212–10290
2. Zirak N, Shirinbayan M, Deligant M, Tcharkhtchi A (2022) Toward polymeric and polymer composites impeller fabrication. Polymers (Basel). Multidisciplinary Digital Publishing Institute 14:97
3. Shakeri Z, Benfriha K, Zirak N, Shirinbayan M (2022) Mechanical strength and shape accuracy optimization of polyamide FFF parts using grey relational analysis. Sci Rep Nature Publishing Group 12:1–17
4. Motas JG, Gorji NE, Nedelcu D, Brabazon D, Quadrini F (2021) XPS, SEM, DSC and nanoindentation characterization of silver nanoparticle-coated biopolymer pellets. Appl Sci. MDPI 11:7706
5. Mukhtarkhanov M, Perveen A, Talamona D (2020) Application of stereolithography based 3D printing technology in investment casting. Micromachines. MDPI 11:946.
6. Lai CQ, Markandan K, Luo B, Lam YC, Chung WC, Chidambaram A (2021) Viscoelastic and high strain rate response of anisotropic graphene-polymer nanocomposites fabricated with stereolithographic 3D printing. Addit Manuf. Elsevier 37:101721.
7. Watters MP, Bernhardt ML (2018) Curing parameters to improve the mechanical properties of stereolithographic printed specimens. Emerald Publishing Limited, Rapid Prototyp J
8. Chantarapanich N, Puttawibul P, Sitthiseripratip K, Sucharitpwatskul S, Chantaweroad S (2013) Study of the mechanical properties of photo-cured epoxy resin fabricated by stereolithography process. Songklanakarin J Sci Technol 35:91–98
9. Dulieu-Barton JM, Fulton MC (2000) Mechanical properties of a typical stereolithography resin. Strain Wiley Online Library 36:81–87
10. Ambrosio D, Gabrion X, Malecot P, Amiot F, Thibaud S (2020) Influence of manufacturing parameters on the mechanical properties of projection stereolithography–manufactured specimens. Int J Adv Manuf Technol Springer 106:265–277
11. Uzcategui AC, Muralidharan A, Ferguson VL, Bryant SJ, McLeod RR (2018) Understanding and improving mechanical properties in 3D printed parts using a dual-cure acrylate-based resin for stereolithography. Adv Eng Mater. Wiley Online Library 20:1800876
12. Pash N, Hayles GC, Hirata D, Kiuchi D (2012) A comparison of manufacturing methods, accuracy, quality control and testing methods a they relate to high head low flow impeller efficiency and overall compressor performance. Proc 41st Turbomach Symp. Texas A&M University. Turbomachinery Laboratories
13. Chockalingam K, Jawahar N, Chandrasekhar U (2006) Influence of layer thickness on mechanical properties in stereolithography. Emerald Group Publishing Limited, Rapid Prototyp J
14. Fernández-Abia AI, Barreiro J, López de Lacalle LN, Martínez-Pellitero S (2012) Behavior of austenitic stainless steels at high speed turning using specific force coefficients. Int J Adv Manuf Technol Springer 62:505–15
15. Pérez-Ruiz JD, de Lacalle LNL, Urbikain G, Pereira O, Martínez S, Bris J (2021) On the relationship between cutting forces and anisotropy features in the milling of LPBF Inconel 718 for near net shape parts. Int J Mach Tools Manuf Elsevier 170:103801
16. Siviour CR, Jordan JL (2016) High strain rate mechanics of polymers: a review. J Dyn Behav Mater Springer 2:15–32
17. Habib F, Iovenitti P, Masood S, Nikzad M, Ruan D (2019) Design and evaluation of 3D printed polymeric cellular materials for dynamic energy absorption. Int J Adv Manuf Technol Springer 103:2347–2361
18. Mae H, Omiya M, Kishimoto K (2008) Effects of strain rate and density on tensile behavior of polypropylene syntactic foam with polymer microballoons. Mater Sci Eng A Elsevier 477:168–178
19. Brown EN, Rae PJ, Orler EB (2006) The influence of temperature and strain rate on the constitutive and damage responses of polychlorotrifluoroethylene (PCTFE, Kel-F 81). Polymer (Guildf). Elsevier 47:7506–18
20. Arruda EM, Boyce MC, Jayachandran R (1995) Effects of strain rate, temperature and thermomechanical coupling on the finite strain deformation of glassy polymers. Mech Mater Elsevier 19:193–212
21. Kendall MJ, Siviour CR (2013) Experimentally simulating adiabatic conditions: approximating high rate polymer behavior using low rate experiments with temperature profiles. Polymer (Guildf). Elsevier 54:5058–63

22. Gerlach R, Siviour CR, Petrinic N, Wiegand J (2008) Experimental characterisation and constitutive modelling of RTM-6 resin under impact loading. Polymer (Guildf). Elsevier 49:2728–37
23. Miedzińska D, Gieleta R, Małek E (2020) Experimental study of strength properties of SLA resins under low and high strain rates. Mech Mater. Elsevier 141:103245
24. Martín-Montal J, Pernas-Sánchez J, Varas D (2021) Experimental characterization framework for SLA additive manufacturing materials. Polymers (Basel). Multidisciplinary Digital Publishing Institute 13:1147
25. Abbasnezhad N, Khavandi A, Fitoussi J, Arabi H, Shirinbayan M, Tcharkhtchi A (2018) Influence of loading conditions on the overall mechanical behavior of polyether-ether-ketone (PEEK). Int J Fatigue Elsevier 109:83–92
26. Gilat A, Goldberg RK, Roberts GD (2007) Strain rate sensitivity of epoxy resin in tensile and shear loading. J Aerosp Eng. Am Soc Civil Eng 20:75–89
27. Somarathna H, Raman SN, Mohotti D, Mutalib AA, Badri KH (2020) Rate dependent tensile behavior of polyurethane under varying strain rates. Constr Build Mater Elsevier 254:119203
28. Shirinbayan M, Fitoussi J, Abbasnezhad N, Meraghni F, Surowiec B, Tcharkhtchi A (2017) Mechanical characterization of a Low density sheet molding compound (LD-SMC): multi-scale damage analysis and strain rate effect. Compos Part B Eng 131:8–20
29. Shirinbayan M, Fitoussi J, Meraghni F, Surowiec B, Bocquet M, Tcharkhtchi A (2015) High strain rate visco-damageable behavior of advanced sheet molding compound (A-SMC) under tension. Compos Part B Eng Elsevier Ltd 82:30–41
30. Fitoussi J, Nikooharf MH, Kallel A, Shirinbayan M (2022) Mechanical properties and damage behavior of polypropylene composite (GF50-PP) plate fabricated by thermocompression process under high strain rate loading at room and cryogenic temperatures. Appl Compos Mater Springer 29:1959–1979
31. Siviour CR, Walley SM, Proud WG, Field JE (2005) The high strain rate compressive behaviour of polycarbonate and polyvinylidene difluoride. Polymer (Guildf) [Internet]. 46:12546–55. Available from: https://www.sciencedirect.com/science/article/pii/S0032386105015806
32. Hund J, Granum HM, Olufsen SN, Holmström PH, Johnsen J, Clausen AH (2022) Impact of stress triaxiality, strain rate, and temperature on the mechanical response and morphology of PVDF. Polym Test. Elsevier 114:107717
33. Miao Y, Du W, Yin J, Zeng Y, Wang C (2022) Characterizing multi mechanical behaviors for epoxy-like materials under wide strain rate range. Polym Test. Elsevier 107804
34. Zhang H, Chang H, Li X, Wu X, He Q (2022) The effect of strain rate on compressive behavior and failure mechanism of CMDB propellant. Def Technol. Elsevier 18:467–475